Wall Effects of Laminar Hydrogen Flames over Platinum and Inert Surfaces

Johan C. G. Andrae and Pehr H. Björnbom
Dept. of Chemical Engineering and Technology, Royal Institute of Technology, SE-100 44 Stockholm, Sweden

Different aspects of wall effects in the combustion of lean, laminar and stationary hydrogen flames in an axisymmetric boundary-layer flow were studied using numerical simulations with the program CRESLAF. The importance of the chemical wall effects compared to thermal wall effects caused by heat transfer to a cold wall was investigated in the reaction zone by using different combustion systems at atmospheric pressure. Surface mechanisms include a catalytic surface, an inert surface that promotes radical recombinations, and a completely inert wall used as reference was the simplest possible boundary condition. The analysis of the results show that for the richer combustion case ($\phi = 0.5$) the surface chemistry gives significant wall effects, while the thermal and velocity boundary layer gives rather small effects. But for the leaner combustion case ($\phi = 0.1$) the thermal and velocity boundary layer gives more significant wall effects, while surface chemistry gives less significant wall effects compared to the other case. As expected, the overall wall effects were more pronounced for the leaner combustion case.

Introduction

Studying the nature of the flame–wall interaction is important for both the understanding of fundamental combustion processes and improving the efficiency of engines.

In contrast to traditional engines, where the heat from the flame is sufficient to keep wall effects down, in lean combustion the effects of the cooled wall are significant. In a lean-combustion engine the fuel may be injected close to the ignition device in order to obtain a richer fuel mixture close to this device, but this means even leaner conditions in other parts of the combustion chamber. This may give rise to problems such that the flame goes out due to the cold wall or to incomplete combustion of the fuel near the wall, with subsequent emissions of unburned hydrocarbons. The complex interactions in near-wall combustion are not well understood. Some of the complicating effects are, for example, unsteady boundary layers, nonuniform wall temperatures, and piston-induced fluid motion (Popp and Baum, 1997).

The effects of the cooled wall may be due to the decrease in temperature across the thermal boundary layer, free-radical chain termination on the wall that is more pronounced at lower temperatures (Westbrook et al., 1981), or a combination of these.

It is not well known which of the effects just mentioned dominate, but surface diffusion brings radicals together, which assists radical recombination (Aghalayam et al., 1998). Despite the low mol fraction, quenching out of radicals has been shown to retard combustion at ignition solely due to the kinetics of the surface reactions (Aghalayam et al., 1998). But as a consequence of the extremely low reactivity due to the low mol fractions, the high temperatures of the surface reactions did not play a significant role at ignition.

In previous studies one-dimensional stagnation point-flow geometry has most commonly been investigated (such as Popp and Baum, 1997; Aghalayam et al., 1998). However, for a flame propagating along a wall, for example, in engines when the flame moves across the piston head and cylinder head, two- or three-dimensional effects may be important. In this study we therefore have used the program CRESLAF (Coltrin et al., 1993) to numerically investigate wall effects of steady-state H_2 flames in a boundary-layer flow, and specially the kinetic and thermal effects that the cooled wall give rise to. We have used different wall boundary conditions for the combustion of hydrogen in order to address questions

Correspondence concerning this article should be addressed to J. C. G. Andrae.

such as which part of the wall effects is most important at a given set of conditions. Unlike previous studies in the literature, we have made an analysis where wall kinetics parameters, wall temperature, and gas-phase transport parameters have been varied in order to elucidate those problems.

The Model

There are two significant flow configurations in flame quenching, the side-wall and the head-on (that is, stagnation) configuration (Cleary and Farrel, 1995). To describe the side-wall quenching, two-dimensional (2-D) boundary-layer flow geometry is used coupled with a detailed description of the chemical reaction in the gas-phase and on the surface. The 2-D calculations were conducted using the program CRESLAF (Coltrin et al., 1993). CRESLAF, which runs in conjunction with CHEMKIN (Kee et al., 1996), SURFACE CHEMKIN (Coltrin et al., 1996), as well as the CHEMKIN transport data base (Kee et al., 1986), solves the boundary-layer equations that describe the fluid flow, coupled with species equations describing the chemical reaction and both convective and diffusive transport of species. In the principal flow direction, and consistent with the boundary layer assumption, diffusive transport is neglected compared with the convective transport. The mathematical description of a boundary layer over a flat plate is given in detail elsewhere (Coltrin et al., 1986). The inlet gas-composition and temperature to the defined reactor are independent of the distance normal to the wall, and the normal velocity component is zero. The wall is nonadiabatic with first a linearly decreasing temperature, and then a constant temperature. In the calculations we consider a symmetric channel at atmospheric pressure in planar coordinates that is 1 cm long and 1 cm high from the symmetry line. The simulations are run on a grid of 70 nodes in the radial direction, on a Digital Alpha Unix machine. After comparison with 140 and 200 mesh points, this discretization of the grid was found to give satisfactory resolution. The typical CPU time required for the simulations was approximately 3 1/2 min.

Chemical Kinetic Models

Gas-phase chemistry

In our simulations, we have used the gas-phase mechanism given in Table 1 taken from Giovangigli and Smooke (1987). The units of the preexponential factor A are in moles, cm^3, and s. Terms E, R, and T are the activation energy, the universal gas constant, and the temperature, respectively. The mechanism is formulated with the CHEMKIN software (Kee et al., 1996). We apply it in this work with modifications in reactions 9 and 11 (see the subsection titled ''Initial Conditions'' later in this article).

Table 1. Gas-Phase Reaction Mechanism for Hydrogen–Air

No.	Reactions	A (mol,cm,s)	n	E (kJ/mol)
1.	$H+O_2=O+OH$	5.1×10^{16}	−0.82	69.1
2.	$H_2+O=H+OH$	1.8×10^{10}	1.0	37.0
3.	$H_2+OH=H_2O+H$	1.2×10^{9}	1.3	15.2
4.	$OH+OH=H_2O+O$	6.0×10^{8}	1.3	0.0
5.	$H_2+O_2=OH+OH$	1.7×10^{13}	0.0	200.0
6.	$H+OH+M=H_2O+M^*$	7.5×10^{23}	−2.6	0.0
7.	$O_2+M=O+O+M$	1.9×10^{11}	0.5	400.1
8	$H_2+M=H+H+M^{**}$	2.2×10^{12}	0.5	387.7
9.	$H+O_2+M=HO_2+M^{\dagger\ddagger}$	2.1×10^{18}	−1.0	0.0
10.	$H+O_2+O_2=HO_2+O_2$	6.7×10^{19}	−1.42	0.0
11.	$H+O_2+N_2=HO_2+N_2^{\ddagger}$	6.7×10^{19}	−1.42	0.0
12.	$HO_2+H=H_2+O_2$	2.5×10^{13}	0.0	2.9
13.	$HO_2+H=OH+OH$	2.5×10^{14}	0.0	7.9
14.	$HO_2+O=OH+O_2$	4.8×10^{13}	0.0	4.2
15.	$HO_2+OH=H_2O+O_2$	5.0×10^{13}	0.0	4.2
16.	$HO_2+HO_2=H_2O_2+O_2$	2.0×10^{12}	0.0	0.0
17.	$H_2O_2+M=OH+OH+M$	1.2×10^{17}	0.0	190.5
18.	$H_2O_2+H=HO_2+H_2$	1.7×10^{12}	0.0	15.7
19.	$H_2O_2+OH=H_2O+HO_2$	1.0×10^{13}	0.0	7.5

Source: V. Giovangigli and M. D. Smooke, *Combust. Sci. Tech.*, 1987.
Note: The rate constant is computed using the modified Arrhenius expression $k=AT^n\exp(-E/RT)$.
Third-body enhancement factors:
$^*H_2O/20.0/$.
$^{**}H_2O/6.0/\quad H/2.0/\quad H_2/3.0/$.
$^{\dagger}H_2O/21.0/\quad H_2/3.3/\quad O_2/0.0/\quad N_2/0.0/$.
$^{\ddagger}N_2$ is substituted by He in the calculations.

Surface chemistry

The SURFACE CHEMKIN software (Coltrin et al., 1996) is used for the formulation of the surface mechanisms. To describe the interaction of the flame with the wall, we have used two different surface mechanisms in our simulations: one on platinum and the other on an inert wall promoting radical recombinations. For platinum, we used a developed surface mechanism previously used in a boundary layer (Warnatz et al., 1994; Hellsing et al., 1987), shown in Table 2, where we have added the H_2O_2 and HO_2 reactions (No. 12 and No. 13). The surface density of the platinum surface was 2.71×10^{-9} mol/cm^2. It should be noted that in recent years surface reaction mechanisms that better predict the species cov-

Table 2. Surface Reaction Mechanism on Pt for Hydrogen Oxidation

No.	Reactions	A (cm,mol,s)	E (kJ/mol)	
1.	$H_2+Pt(S)=H_2(S)$	0.05	0.0	Sticking coefficient
2.	$H_2(S)+Pt(S)=H(S)+H(S)$	7.50×10^{22}	15.6	Rate coefficient
3.	$O_2+Pt(S)=O_2(S)$	0.023	0.0	Sticking coefficient
4.	$O_2(S)+Pt(S)=O(S)+O(S)$	2.50×10^{24}	0.0	Rate coefficient
5.	$H(S)+O(S)=OH(S)+Pt(S)$	3.70×10^{21}	19.3	Rate coefficient
6.	$H(S)+OH(S)=H_2O(S)+O(S)$	3.70×10^{21}	0.0	Rate coefficient
7.	$OH(S)+OH(S)=H_2O(S)+O(S)$	3.70×10^{24}	100.5	Rate coefficient
8.	$H+Pt(S)=H(S)$	1.00	0.0	Sticking coefficient
9.	$O+Pt(S)=O(S)$	1.00	0.0	Sticking coefficient
10.	$H_2O+Pt(S)=H_2O(S)$	0.75	0.0	Sticking coefficient
11.	$OH+Pt(S)=OH(S)$	1.00	0.0	Sticking coefficient
12.	$H_2O_2+Pt(S)=OH(S)+OH(S)$	1.00	0.0	Sticking coefficient
13.	$HO_2+Pt(S)=OH(S)+O(S)$	1.00	0.0	Sticking coefficient

Table 3. Surface Reaction Mechanism on Inert Wall for Hydrogen Oxidation

No.	Reactions	A (cm,mol,s)	E (kJ/mol)	
1.	$H + S \rightarrow H(S)$	1.00	0.0	Sticking coefficient
2.	$2\,H(S) \rightarrow H_2 + 2S$	1×10^{13}	0.0	Rate coefficient
3.	$O + S \rightarrow O(S)$	1.00	0.0	Sticking coefficient
4.	$2\,O(S) \rightarrow O_2 + 2S$	1×10^{13}	0.0	Rate coefficient
5.	$OH + S \rightarrow OH(S)$	1.0	0.0	Sticking coefficient
6.	$2\,OH(S) \rightarrow H_2O + O(S) + S$	1×10^{13}	0.0	Rate coefficient
7.	$2\,O(S) \rightarrow O_2 + 2S$	1×10^{13}	0.0	Rate coefficient
8.	$HO_2 + {}_2(S) \rightarrow OH(S) + O(S)$	1.0	0.0	Sticking coefficient
9.	$2\,OH(S) \rightarrow H_2O + O(S) + S$	1×10^{13}	0.0	Rate coefficient
10.	$2\,O(S) \rightarrow O_2 + 2S$	1×10^{13}	0.0	Rate coefficient
11.	$H_2O_2 + 2(S) \rightarrow 2\,OH(S)$	1.0	0.0	Sticking coefficient
12.	$2\,OH(S) \rightarrow H_2O + O(S) + S$	1×10^{13}	0.0	Rate coefficient
13.	$2\,O(S) \rightarrow O_2 + 2(S)$	1×10^{13}	0.0	Rate coefficient

erages have been developed (such as Park et al., 1999).

For reactions taking place on inert walls, we have used the mechanism shown in Table 3 that was used in work with stagnation-point flow geometries (Aghalayam et al., 1998).

Here the surface acts like a sink for the radicals and adsorbs them, and the recombination on the surface leads to a stable species that desorbs into the gas phase.

Here S denotes a vacant surface site, and $H(S)$ the adsorbed surface species. The surface site density was set to 4.17×10^{-7} mol/cm^2.

Initial Conditions. The calculations were performed at atmospheric pressure for lean H_2/air mixtures with fuel equivalence ratios, ϕ, of 0.5 and 0.1. The unburned gases were preheated to a temperature of 975 K and had an inlet velocity of 900 cm/s. For this small-size reactor, these conditions produced gas ignition and a clear shape of the reaction zone that was desirable for investigating the wall boundary layer. To investigate the influence of heat and mass transfer on the overall wall effects, we changed the carrier gas from nitrogen to helium. The heat conduction and diffusivity of helium is higher than that of nitrogen, but it has a lower heat capacity. To compensate for that lower heat capacity, we also changed the thermodynamic data of helium in the CHEMKIN thermodynamic database (Kee et al., 1990) to those of nitrogen.

Boundary Conditions. If x denotes the distance along the principal flow direction, at the inlet to the reactor ($x = 0$) the temperature of the unburned gases, T_{in}, is the same as the wall temperature, T_w (that is, $T_{in} = T_w$). The wall temperature is formulated in a way that the temperature decreases linearly from T_{in} at $x = 0$ to T_w at $x = 0.5$ cm (that is, the wall temperature partly varies in the reaction zone). Wall temperatures used were 400 K and 600 K. At the inlet to the reactor, the velocity profile is flat with a boundary-layer thickness of 0.01 cm (within which the velocity profile is parabolic). The boundary layer then develops very fast downstream in the channel.

Table 4 contains the different combinations of gas phase and surface mechanisms used in the calculations together with their acronyms. A recombination surface is treated (Table 3), that is, a surface that promotes recombination of unstable species such as OH, O, H, H_2O_2, and HO_2. We also treat the catalytic combustion of H_2 on Pt (Table 2). As a reference we use a completely inert wall (no surface reactions or species).

Results and Discussion

The present investigation concerns a type of flow field with flow parallel to the wall that may occur in some parts of automotive engines and in the combustion chambers of gas turbines. Our use of laminar flow would be a restriction compared to real conditions, where turbulent flow conditions are most common. However, there will always be a laminar sublayer close to the wall in turbulent flow. This suggests that results obtained for laminar flow fields may also be valid, to a certain extent, in the case of turbulent flow conditions. In general, the heat- and mass-transfer rates would be higher in a turbulent boundary layer than in a laminar boundary layer. This should enhance wall effects in the case of turbulent boundary layers as opposed to laminar ones.

In the present investigation we have compared walls with different properties. We want to see the effect of these property changes in order to elucidate the importance of the chemical wall effects, if they occur, compared to thermal wall effects caused by heat transfer to a cold wall.

We have studied a wall (Pt) that causes catalytic combustion, a wall that causes free radicals to recombine (Rr), and a completely chemically inert wall (In).

Real walls may vary and can, for example, consist of a more or less pure metal surface or a metal surface covered by an oil film. This means that the chemical properties of real walls may well vary within the range we have chosen to study. One important reason for choosing Pt as a wall material with a catalytic combustion property is that this is the only wall material for which the surface reaction mechanism and kinetics are reasonably well understood (Vlachos, 1996; Warnatz et al., 1994; Hellsing et al., 1987).

Another method we have used to try to elucidate the effects of mass and heat transfer is to substitute nitrogen for modified helium. This would enhance mass- and heat-trans-

Table 4. Combinations of Gas and Surface Mechanisms Used in the Calculations

Surface Mechanism	Carrier Gas N_2	Modified He*
Platinum (Table 2)	PtN_2	PtHe
Recombinations (Table 3)	RrN_2	RrHe
Inert wall	InN_2	InHe

* He with the same heat capacity as N_2.
PtN_2: acronym for the combination Pt wall-carrier gas N_2, etc.

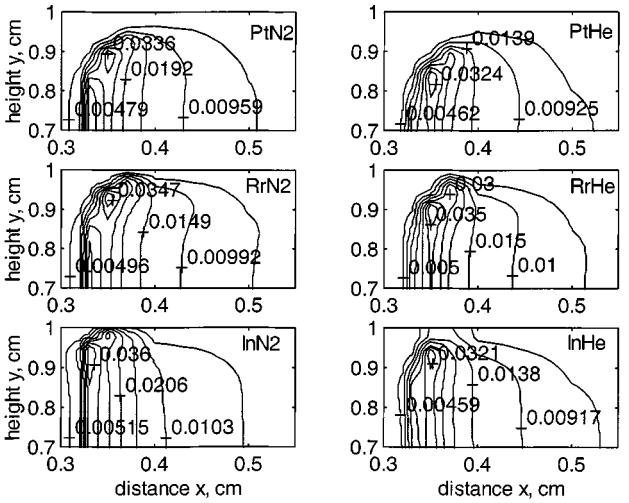

Figure 1. Contour of the *H* radical concentration (mol fractions) for the combustion systems in Table 4.

$\phi = 0.5$; $T_w = 600$ K; $T_{in} = 975$ K.

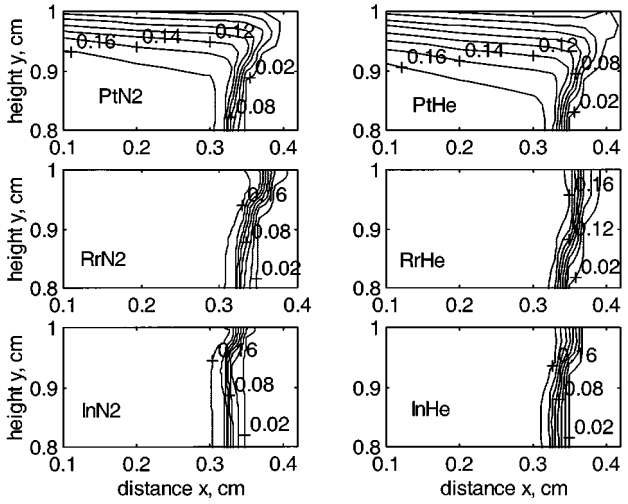

Figure 3. Contour of the H_2 concentration (mol fractions) for the combustion systems in Table 4.

$\phi = 0.5$, $T_w = 600$ K; $T_{in} = 975$ K.

fer rates that are due to the higher diffusivity and heat conductivity in modified helium compared to nitrogen.

Contour profiles of the atomic hydrogen concentration, hydrogen concentration, temperature, and velocity for the two equivalence ratios are shown in Figures 1–8 for all combinations of the three wall materials and the two carrier gas compositions named in Table 4. In these plots y denotes the height above the symmetry line ($y = 0$ cm in the middle of the channel and $y = 1$ cm at the wall). The wall temperature profile is the same in all plots. The hydrogen atom concentration is a measure of the overall combustion rate and therefore indicates the shape and position of the reaction zone. For different wall conditions, but with the same initial conditions, the reaction zone appeared at the same position in the direction of the flow. This also means that the wall temperature at the reaction zone was the same in all such cases.

The diagrams for the inert wall material (InN_2 and InHe in Table 4) give us information on the extent of the wall effects due to heat transfer combined with the effect of no slip at the wall, and the development of the boundary layer compared to a free flame.

There is a large part of the channel where the reaction rate is totally unaffected by the wall. The size of this central portion is apparent from the contour plots. For example, according Figure 1, the H-atom concentration profiles within the reaction zone are flat at about 8 mm from the middle of the channel, while they are affected by the wall in an area within 2 mm from the wall.

In a large central portion of the channel, the velocity profile is flat. In the reaction zone in this part of the channel,

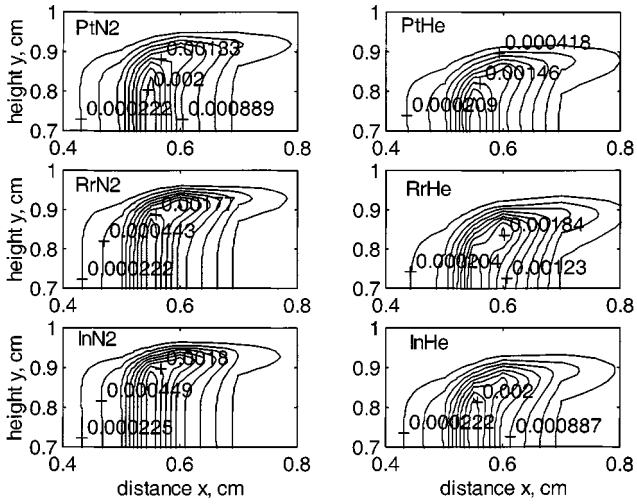

Figure 2. Contour of the *H* radical concentration (mol fractions) for the combustion systems in Table 4.

$\phi = 0.1$; $T_w = 600$ K; $T_{in} = 975$ K.

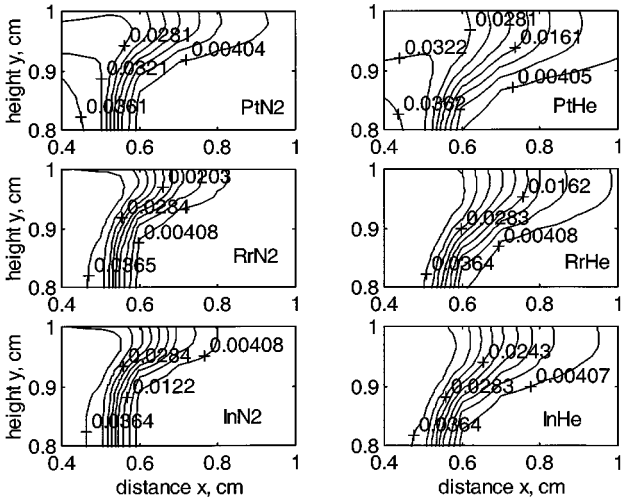

Figure 4. Contour of the H_2 concentration (mol fractions) for the combustion systems in Table 4.

$\phi = 0.1$; $T_w = 600$ K; $T_{in} = 975$ K.

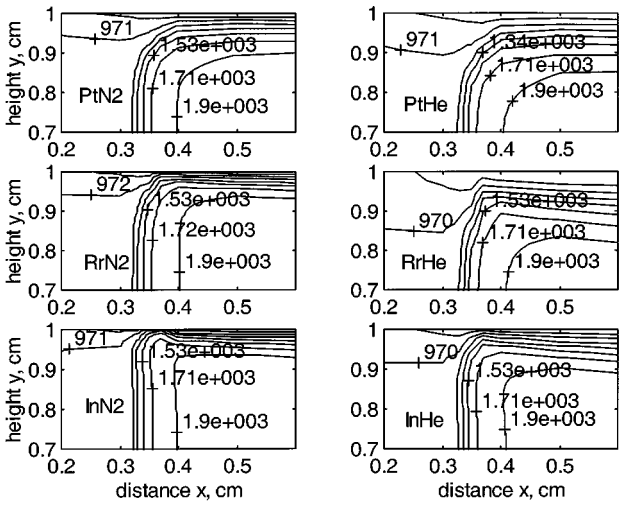

Figure 5. Contour of the temperature (K) for the combustion systems in Table 4.

$\phi = 0.5$; $T_w = 600$ K; $T_{in} = 975$ K.

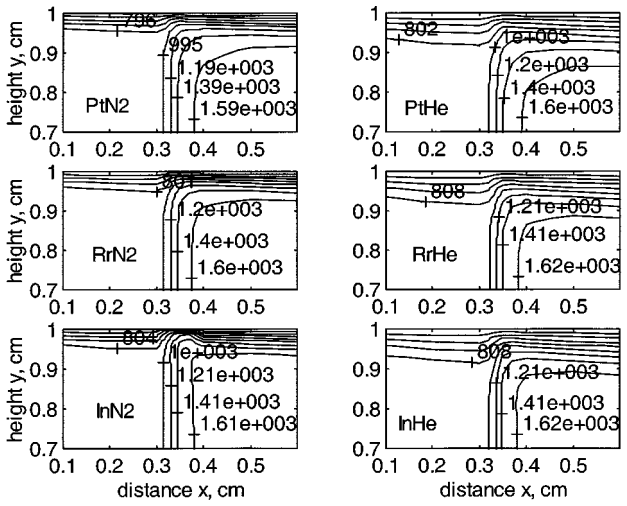

Figure 7. Contour plots of the velocity (cm/s) for the combustion systems in Table 4.

$\phi = 0.5$; $T_w = 600$ K; $T_{in} = 975$ K.

the concentrations and temperature profiles also are flat without any influence from the wall. In this section the reaction rate is always perpendicular to the flow due to the equalizing effect of diffusion and heat conduction in that direction.

This section of the channel is not interesting in our context, but we consider the boundary layer at the wall where velocity, temperature, and concentrations strongly vary with the distance from the wall.

The wall effects are the changes in the combustion process caused by the processes in this boundary layer compared to an imaginary combustion process without any boundary layer. The width of the central part with flat profiles is about 16 mm in our case, but this measure is really not important. In our calculations, the thickness of the boundary layer in the reaction zone is 1–2 mm. The contour plots in Figures 1–8 emphasize the boundary layers within the reaction zone and show a section of the channel that includes a distance of 2–3 mm outward from the wall and an axial distance of 3–6 mm around the reaction zone.

Obviously, the falling temperature causes a considerable decrease in reaction rate close to the wall. The highest H concentration at the wall is less than 50% of its maximum value in the reaction zone.

Obviously the wall effects at inert walls are due to the combination of heat transfer and the development of the boundary layer compared to a free flame.

For $\phi = 0.5$, the wall effects at inert walls are fairly small, especially the effect on the H_2 conversion (see Figure 3). When the wall material is changed to a material that affords recombination of radicals, there is a decrease in the H concentration close to the wall. The effect of the wall is seen farther from the wall than it is in the case of an inert wall

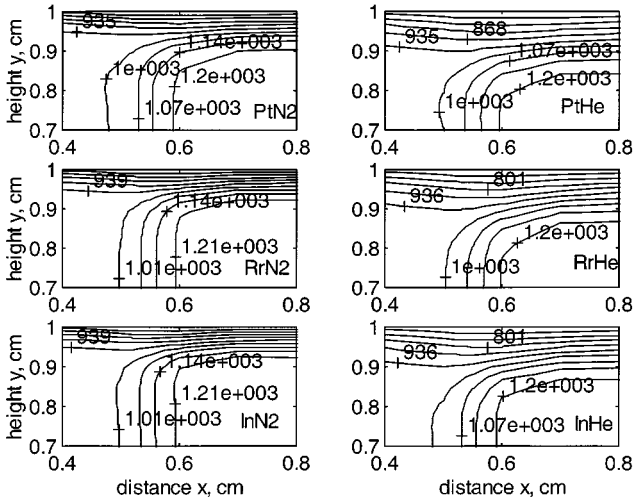

Figure 6. Contour of the temperature (K) for the combustion systems in Table 4.

$\phi = 0.1$; $T_w = 600$ K; $T_{in} = 975$ K.

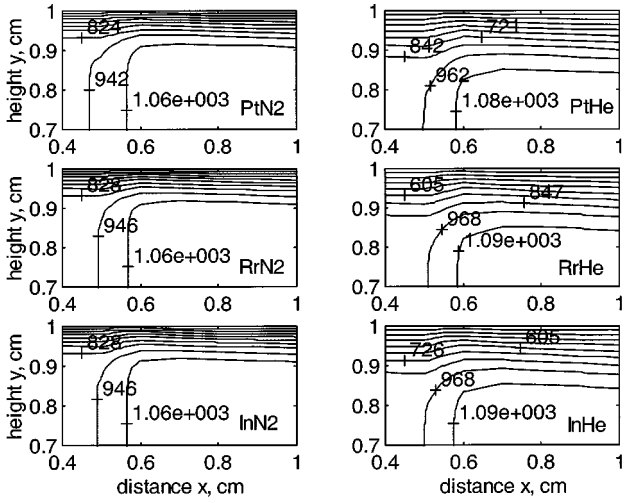

Figure 8. Contour plots of the velocity (cm/s) for the combustion systems in Table 4.

$\phi = 0.1$; $T_w = 600$ K; $T_{in} = 975$ K.

material. The H concentration at the wall and in the zone close to the wall becomes almost equal to zero (see Figure 1). The effect on H_2 conversion is still small but significant (see Figure 3). However, the general structure of the reaction zone is not changed. With a Pt wall we obtain an even lower H concentration compared with the recombination wall and the inert wall. Here the depletion of H radicals close to the wall is more pronounced than with the recombination surface (see Figure 1).

The more pronounced depletion of H radicals in the Pt-wall case compared to a recombination wall may have three causes. The first one is the net adsorption of the H radicals on the wall being higher for Pt than for the recombination wall. The second is the depletion of hydrogen in the boundary layer due to catalytic combustion on Pt resulting in the lower production of H radicals in this layer. The third is increased H-radical recombination in the boundary layer due the third body effect caused by the high water concentration in this layer. This high concentration is due to the production of water by the catalytic combustion on the Pt wall. The latter type of product inhibition for H_2 as fuel was previously found for stagnation-point flow geometry (Vlachos, 1996; Bui et al., 1996).

Our H-concentrations plots suggest the third cause, that is, increased H-radical recombination due the third-body effect of water. It cannot be the first one, since H-radical adsorption is slower on Pt than on the recombination wall.

This can be seen since the rate of H-radical adsorption is proportional to the H-radical concentration gradient near the wall and, according to our contour plots (Figure 1), this gradient is much less for the Pt wall than for the recombination wall. The second cause, hydrogen depletion, can be excluded by comparing the contour plots for the H-radical concentration (Figure 1) and the contour plots for hydrogen concentration (Figure 3). This comparison shows that the H-radical concentrations are more depleted for the Pt wall than for the recombination wall, as well as in parts of the boundary layer without hydrogen depletion. This would not be the case if hydrogen depletion was the cause of the excessive H-radical depletion in the Pt-wall case. Furthermore, more unburnt hydrogen is left in the Pt-wall case than in that of a recombination wall.

The effect of changing the carrier gas from nitrogen to modified helium can be seen in Figures 5 and 7. The boundary layers become thicker when helium is the carrier gas, as would be expected, due to the gas's higher heat conductivity and diffusivity. But, when changing from N_2 to modified He (see Figure 1), the same differences remain in the H-molar concentration profile near the wall for the three wall materials. This indicates that it is the chemical interactions on the wall that give rise to most of the wall effects when $\phi = 0.5$.

When the surface temperature is decreased to 400 K, the same trends can be seen as for when the wall temperature is 600 K, except that now the H-atom concentrations have significantly decreased. This also agrees with when the chemical interaction with the wall is pronounced at $\phi = 0.5$. On the other hand, the effect on unburned H_2 was minor when the wall temperature was decreased.

As the fuel equivalence ratio is decreased to 0.1, the situation changes. A significant difference compared to the richer combustion case is found for the inert surface material (In). Here the H concentration close to the wall has become almost zero, and the differences between the three wall materials has become small (see Figure 2). Also, the thermal and velocity boundary layer has become thicker compared to when $\phi = 0.5$ (see Figures 6 and 8). This indicates that heat and momentum transport have become more important for the wall effects. The H_2 profiles are shown in Figure 4. They have become more similar for different wall materials than in the richer case. This means that the combination is less affected by the reactions on the wall, and also indicates that the thermal wall effects have become more important than the chemical wall effects. Consequently, a pronounced increase in unburnt H_2 in the boundary layer occurred when the wall temperature was decreased from 600 K to 400 K. However, the effect on H-atom concentrations was minor. In Figure 4, it can also be seen from the H_2 profiles that the overall effects from the wall are more pronounced (that is, a lower conversion) at $\phi = 0.1$ than at $\phi = 0.5$. This is as would be expected. A lower concentration of fuel near the wall gives a lower reaction rate, and therefore is more easily affected by disturbances from the wall. These wall effects are mainly thermal.

Conclusions

The importance of the chemical wall effects compared to thermal wall effects caused by heat transfer to a cold wall have been studied. We investigated the combustion of a lean, laminar, and stationary hydrogen flame in an axisymmetric boundary-layer flow by using different combustion systems at atmospheric pressure.

For the rich combustion case, the thermal and velocity boundary layer produces rather small wall effects, while surface chemistry produces significant wall effects. For the leaner combustion case, the surface chemistry produces less significant wall effects, while the thermal and velocity boundary layer produces more significant wall effects compared to the other case. Also, for the leaner combustion case the overall effects are more pronounced. This is what would be expected.

Acknowledgment

This work is supported financially by CeCoST (The Centre for Combustion Science and Technology) and The Centre of Environmental Science, KTH. The work is part of the CeCoST research program Turbulent Combustion (project PROJ9803-TC). Lennart Edsberg at the department of Numerical Analysis and Computing Science at KTH has played an important part in performing the CRESLAF calculations.

Literature Cited

Aghalayam, P., P.-A. Bui, and D. G. Vlachos, ''The Role of Radical Wall Quenching in Flame Stability and Wall Heat Flux: Hydrogen-Air Mixtures,'' *Combust. Theory Modelling* **2**, 515 (1998).

Bui, P.-A., D. G. Vlachos, and P. R. Westmoreland, ''Homogeneous Ignition of Hydrogen-Air Mixtures over Platinum,'' *Proc. Symp.* (*International*) *on Combustion*, p. 1763 (1996).

Cleary, D. J., and P. V. Farrel, ''Single Surface Flame Quenching Distance Dependence on Wall Temperature, Quenching Geometry and Turbulence,'' *Proc. Soc. Automot. Eng. Int. Congress and Exposition*, Detroit, MI, p. 49 (1995).

Coltrin, M. E., R. J. Kee, and J. A. Miller, ''A Mathematical Model of Silicon Chemical Vapor Deposition,'' *J. Electrochem. Soc.*, **133**, 1206 (1986).

Coltrin, M. E., K. Moffat, R. J. Kee, and F. M. Rupley, ''Creslaf (Version 4.0): A Fortran Program for Modeling Laminar, Chemically Reacting Boundary-Layer Flowing Cylindrical or Planar Channels,'' Sandia National Labs. Rep., Sandia National Laboratories, NM (1993).

Coltrin, M. E., R. J. Kee, F. M. Rupley, and E. Meeks, ''Surface Chemkin: III. A Fortran Package for Analyzing Heterogeneous Chemical Kinetics at a Solid Surface-Gas Phase Interface,'' Sandia National Labs. Rep., Sandia National Laboratories, NM (1996).

Giovangigli, V., and M. D. Smooke, ''Extinction of Strained Premixed Laminar Flames with Complex Chemistry,'' *Combust. Sci. Tech*., **53**, 23 (1987).

Hellsing, B., B. Kasemo, S. Ljungström, A. Rosen, and T. Wahnstrom, ''Kinetic Model and Experimental Results for H_2O and OH Production Rates on Pt,'' *Surf. Sci*., **189/190**, 851 (1987).

Kee, R. J., G. Dixon-Lewis, J. Warnatz, M. E. Coltrin, J. A. Miller, and H. K. Moffat, ''A Fortran Computer Code Package for the Evaluation of Gas-Phase, Multicomponent and Transport Properties,'' Sandia National Labs. Rep., Sandia National Laboratories, NM (1986).

Kee, R. J., F. M. Rupley, and J. A. Miller, ''The CHEMKIN Thermodynamic Database,'' Sandia National Labs. Rep., Sandia National Laboratories, NM (1990).

Kee, R. J., F. M. Rupley, E. Meeks, and J. A. Miller, ''Chemkin: III. A Fortran Chemical Kinetics Package for the Analysis of Gas-Phase Chemical and Plasma Kinetics,'' Sandia National Labs. Rep., Sandia National Laboratories, NM (1996).

Park, Y. K., P. Aghalayam, and D. G. Vlachos, ''A Generalized Approach for Predicting Coverage-Dependent Reaction Parameters of Complex Surface Reactions: Application to H_2 Oxidation over Platinum,'' *J. Phys. Chem*. **103**(40), 8101 (1999).

Popp, P., and M. Baum, ''Analysis of Wall Heat Fluxes, Reaction Mechanisms and Unburnt Hydrocarbons during the Head-On Quenching of a Laminar Methane Flame,'' *Combust. Flame*, **108**, 327 (1997).

Vlachos, D. G., ''Homogeneous-Heterogeneous Oxidation Reactions over Platinum and Inert Surfaces,'' *Chem. Eng. Sci*., **51**, 2429 (1996).

Warnatz, J., M. D. Allendorf, R. J. Kee, and M. E. Coltrin, ''A Model of Elementary Chemistry and Fluid Mechanics in the Combustion of Hydrogen on Platinum Surfaces,'' *Combust. Flame*, **96**, 393 (1994).

Westbrook, C. K., A. A. Adamczyk, and A. Lavoie, ''A Numerical Study of Laminar Flame Wall Quenching,'' *Combust. Flame*, **40**, 81 (1981).

Manuscript received Sept. 7, 1999, and revision received Jan. 24, 2000.